

Cell Reports, Volume 28

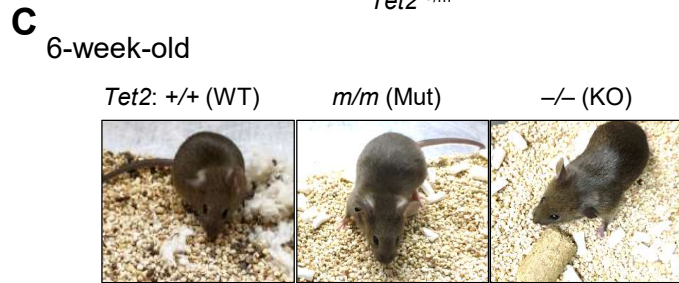
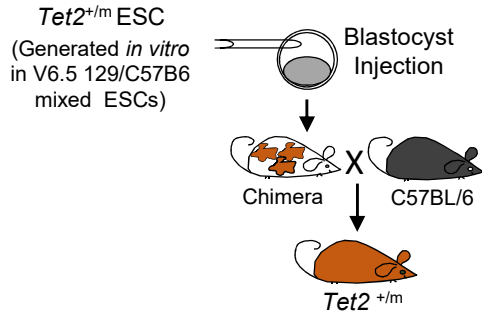
Supplemental Information

**Non-catalytic Roles of Tet2 Are
Essential to Regulate Hematopoietic
Stem and Progenitor Cell Homeostasis**

Kyoko Ito, Joun Lee, Stephanie Chrysanthou, Yilin Zhao, Katherine Josephs, Hiroyo Sato, Julie Teruya-Feldstein, Deyou Zheng, Meelad M. Dawlaty, and Keisuke Ito

A *Tet2* targeting in V6.5 mESCs

mESCs colonies picked & screened	96
Clones heterozygote for <i>m</i> allele (+/ <i>m</i>)	6
+/ <i>m</i> clones with non-intact <i>wt</i> allele	4
Efficiency of proper targeting (2 out of 96)	2%



B *Tet2*^{m/m} mice from *Tet2*^{+/m} X *Tet2*^{+/m} cross

No. of Pups	+/+	+/ <i>m</i>	<i>m/m</i>
65 (10 litters)	20	30	15
Percent (ratio)	30 (1)	46 (2)	23 (1)

Tet2^{-/-} mice from *Tet2*^{+/-} X *Tet2*^{+/-} cross

No. of Pups	+/+	+/-	-/-
79 (10 litters)	23	34	22
Percent (ratio)	29 (1)	43 (2)	27 (1)

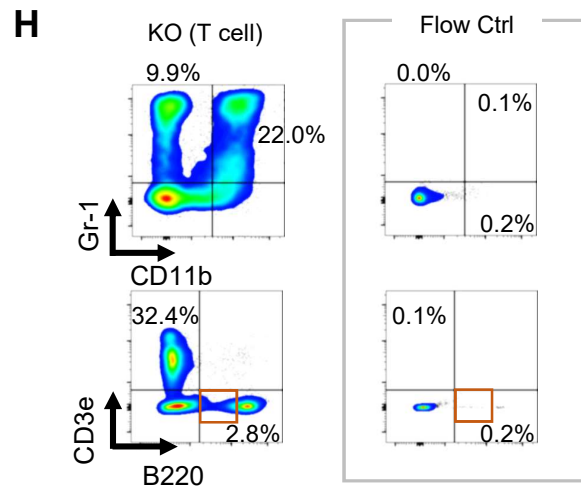
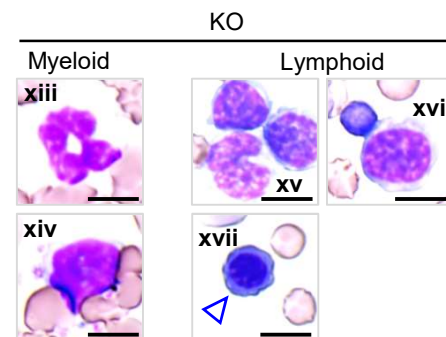
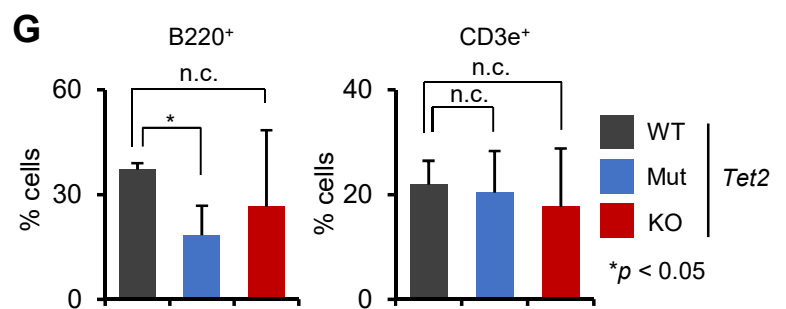
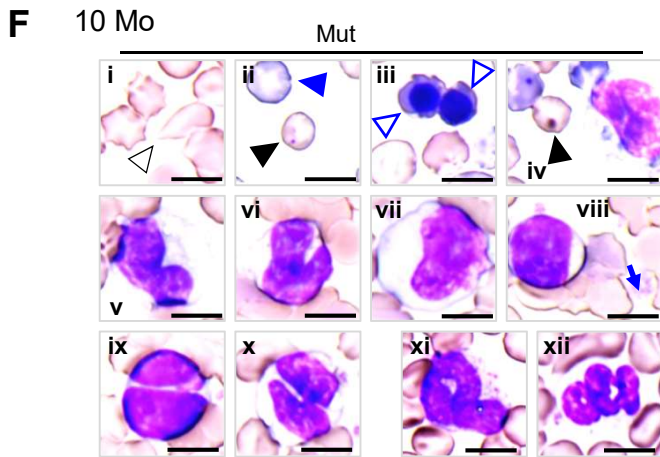
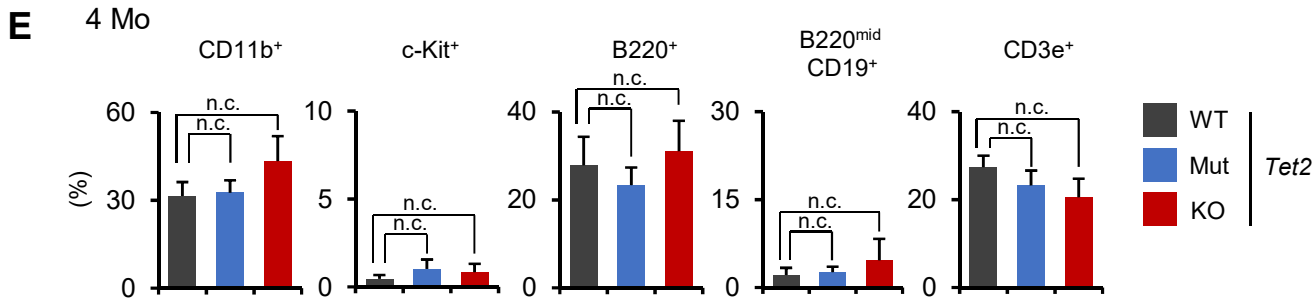
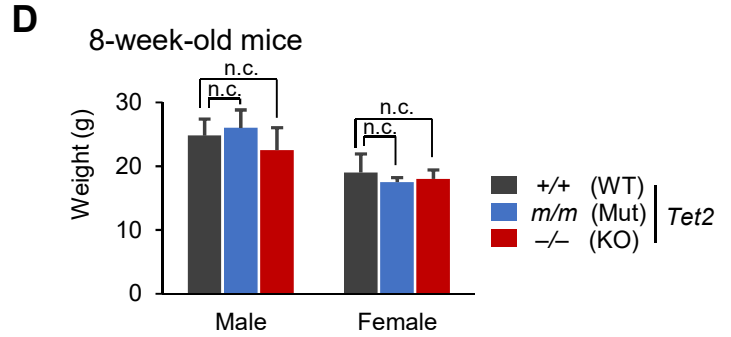


Figure S1 (Related to Figure 1). Generation and hematopoietic characterization of *Tet2* catalytic mutant mice

- (A) Summary of *Tet2* gene-editing in mouse ES cells (top) and schematic of injection of an edited ESC clone into blastocyst to generate *Tet2* catalytic mutant mice.
- (B) Mendelian ratios of *Tet2* catalytic mutant (Mut) and knockout (KO) mice. *Tet2* Mut mice, like knockout mice, are produced at normal mendelian frequency.
- (C) Images of 6-week-old *Tet2* mice of the indicated genotypes.
- (D) Body weight of live *Tet2* Mut and KO mice showing no differences in overall growth in young age.
- (E) Percentages of the indicated fractions in the peripheral blood in *Tet2* Mut and KO mice (4 months old) ($n = 6$).
- (F) Representative images of abnormal hematopoietic cells in PB smears of 10-month-old *Tet2* Mut (i-xii) and KO mice (xiii-xiv, with myeloid disorders; xv-xvii, with lymphoid malignancy). Dysplastic erythroid cells [i-iv, xvii; polychromatophilic (ii, blue arrowhead), Howell-Jolly bodies (ii and iv, black arrowhead), other poikilocytes (e.g. teardrop-shaped dacrocyte and echinocytes) (i, black-outlined arrowhead), and nucleated erythroid cells (iii and xvii, blue-outlined arrowhead). Dysplastic monocytes [v-x and xiv; a pseudo-Pelger-Huet anomaly (ix and x)] and dysplastic platelet (giant platelet) (blue arrow, viii) are shown. Dysplastic neutrophils (xi-xiii) and immature B cells (xv and xvi) are also shown. All images are taken at x100. Scale bars, 10 μ m.
- (G) Percentages of B220⁺ (left) and CD3e⁺ (middle) cells in the PB in *Tet2* Mut and KO mice (10 months old).
- (H) Representative flow data for myeloid and lymphoid lineages in PB from *Tet2* KO mice with T lymphoid phenotypes (10 months old). Unstained flow controls are also shown (right, inset).

Error bars indicate standard deviation. n.c. stands for no significant change.

Figure S2 (Related to Figure 2). Phenotypic and functional characterization of HSPCs from *Tet2* Mut and KO mice

- (A) Percentages of the indicated fractions in the peripheral blood in *Tet2* Mut and KO mice (4 months old) ($n = 6$).
- (B, C) Bone marrow flow analysis for the indicated immature fractions from *Tet2* Mut and KO mice (4 months old, B; 10 months old, C).
- (D) Percentages in live mononuclear cells (left) or relative absolute number (middle, right) of the indicated fractions in the bone marrow in *Tet2* Mut and KO mice (10 months old) ($n = 6$). The alterations of Pro-B and Pre-B are minor in *Tet2* KO mice, while both B-1a fractions and B-1 progenitors are increased.
- (E, F) Colony-forming capacity of HSPCs from 4-month-old *Tet2* Mut and KO mice ($n = 3$) (E). Overview of the experimental design for *in vitro* colony-replating assay (F, left). *Tet2*-KO HSCs have the increased re-plating capacity compared to *Tet2*-Mut HSCs (4 months old, up to 4th round re-plating data, $n = 3$) (F, right).
- (G, H) Profiles of the colonies formed by HSPCs from 10-month-old *Tet2* Mut and KO mice ($n = 3$). Representative images of May-Grünwald-Giemsa–stained cytopsin preparations of the formed-colonies by hematopoietic stem and progenitor cells from *Tet2* Mut and wild-type mice (at 2nd replating) (H). Scale bars, 10 μ m.

HSPCs, hematopoietic stem and progenitor cells; LSK, Lineage⁻cKit⁺Sca1⁺; GMP, granulocyte-monocyte progenitor; CLP, common lymphoid progenitor; Pro-B, Gr-1⁻CD4/8⁻IgM⁻CD43⁺; Pro-B, Gr-1⁻CD4/8⁻IgM⁻CD43⁻; B-1 progenitor, Gr-1⁻CD4/8⁻IgM⁻CD19⁺B220^{dim/-}; GEMM, Colony-forming unit-granulocyte, erythroid, macrophage, and megakaryocyte; GM, Colony-forming unit-granulocyte and macrophage; M, Colony-forming unit-macrophage; E, Burst-forming unit-erythroid. Error bars indicate standard deviation. n.c. stands for no significant change.

Figure S3 (Related to Figure 3). Analysis of spleens from *Tet2* Mut and KO mice

- (A) Representative histologic images of sections of spleen, liver and lymph node from 10-month old *Tet2* Mut mice, stained with H&E. Tissue with myeloid expansion/infiltration are shown (top right for Mut mouse #1, and bottom left for Mut mouse #2). Histologic images of spleen from 10-month old *Tet2* KO mice with B cell phenotypes (bottom right for KO mice #1 and #2, respectively; Magnified spleen image of KO mouse #1, in the inset). Normal tissues in the age-matched wild-type mice are also shown as control (top, left). Scale bars, 250 μ m.
- (B, C) Representative flow data for myeloid and lymphoid lineages in the spleen from *Tet2* Mut and KO mice (4 months old, B left; 10 months old, B right). Percentages of the indicated fractions are also shown ($n = 6$) (C).

Error bars indicate standard deviation. n.c. stands for no significant change.

A

Sample ID	Total no. of reads	After TrimGalore	Trim galore	Alignment (concordant pairs)
KO-1 LSK	33177922	42%	32878550	66.2%
KO-2 LSK	24572563	46%	24353166	67.8%
Mut-1 LSK	27985348	45%	27784460	71.1%
Mut-2 LSK	29234575	45%	29026893	68.9%
WT-1 LSK	22361886	43%	22175751	63.3%
WT-2 LSK	29576940	38%	29322650	63.9%

Sample ID	Total no. of reads	After TrimGalore	Trim galore	Alignment (concordant pairs)
KO-3 Lin ⁻	24823594	42%	24568085	68.7%
KO-4 Lin ⁻	23783109	43%	23610520	68.3%
Mut-5 Lin ⁻	41587013	28%	41206349	69.9%
Mut-6 Lin ⁻	28302608	44%	28012788	68.9%
WT-1 Lin ⁻	26978823	41%	26745245	67.1%
WT-2 Lin ⁻	17932441	44%	17777171	70%

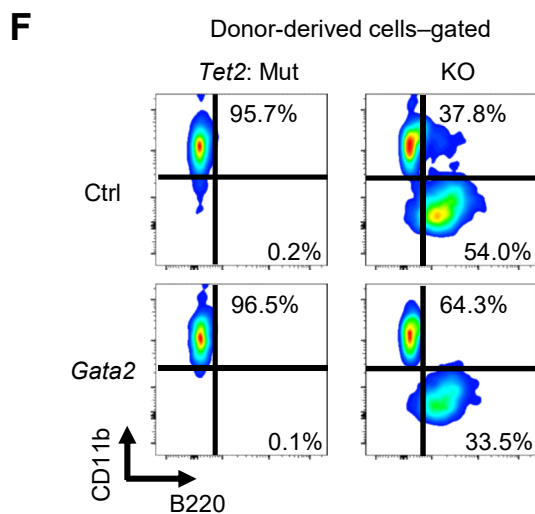
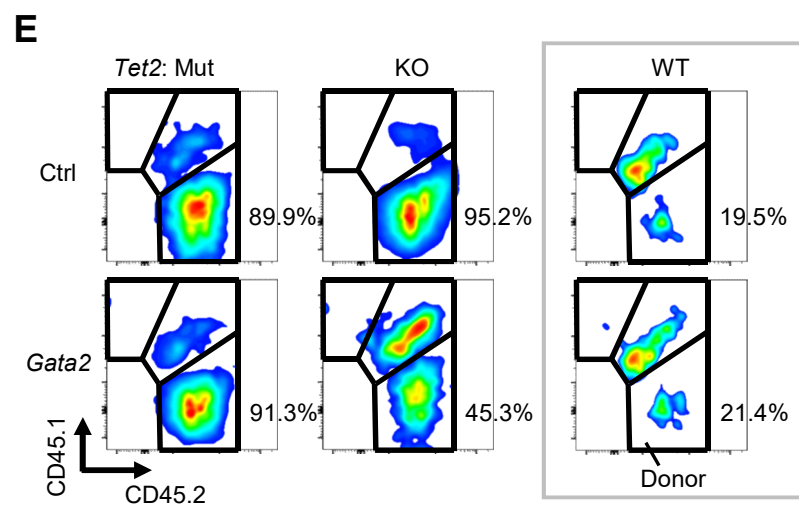
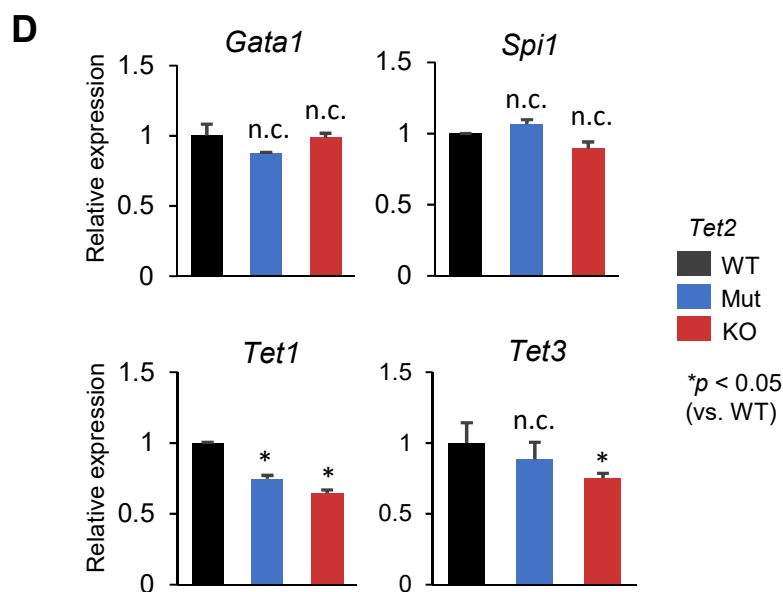
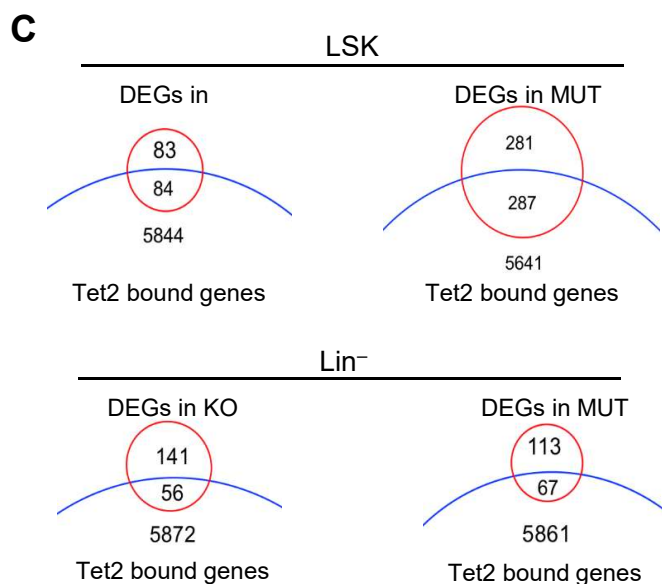
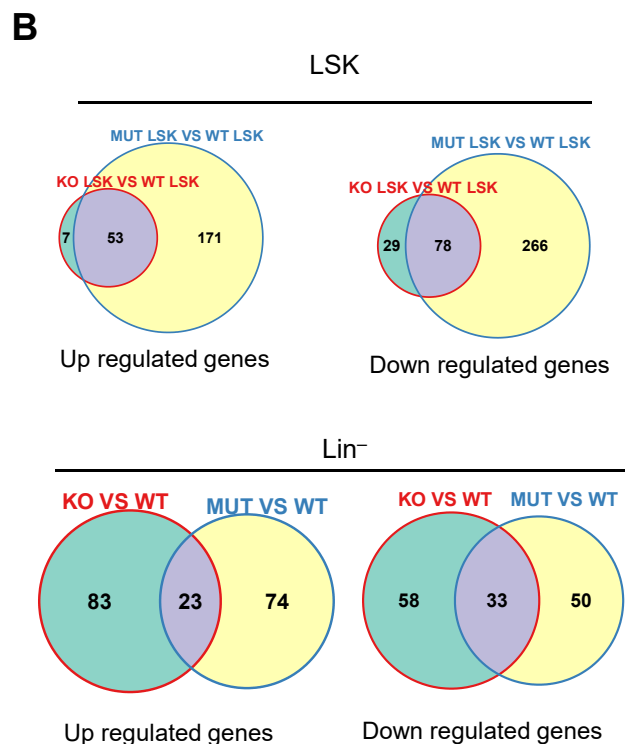


Figure S4 (Related to Figure 4): Gene expression changes in hematopoietic stem and progenitor cells from *Tet2* Mut and KO mice.

- (A) Summary of RNA-seq data.
- (B) Venn diagram of up- and down-regulated DEGs in LSK (left) and Lin⁻ cells (right).
- (C) Venn diagram showing overlap of DEGs with *Tet2* bound genes in bone marrow.
- (D) mRNA levels of indicated genes in LSK cells isolated from 2-month-old mice, quantified by RT-qPCR. Data normalized to *Gapdh*.
- (E, F) Representative flow cytometric analysis for donor-chimerism (E) and CD11b/B220 positivity (F) in peripheral blood of recipient mice transplanted with *Gata2*-expressing *Tet2* Mut bone marrow cells (bottom left) or *Tet2* KO bone marrow cells (bottom right), 3 weeks after BMT. Empty vector transduced controls are also shown (top).

Error bars indicate standard deviation. n.c. stands for no significant change.

Table S1 (Related to STAR Methods): List of oligos, gRNAs and gene blocks used in study

Name	Sequence	Purpose	Source
Tet2 gRNA For oligo	GCATGTTCTGCTGGTCTCTG	Gene targeting	This paper
Tet2 gRNA Rev oligo	CAGAGACCAGCAGAACATGC	Gene targeting	This paper
Tet2 gene block	gcagtggttacgt... 471pb...CCTACAGGGCC...439bp ...tccatacacttaa	Gene targeting	This paper
Tet2 Mut Gen Fw	ATTCTCAGGAGTCACTGCATG	Genotyping Tet2 mutant mice	This paper
Tet2 Mut Gen Rev	TCTATCCATGAAAACACATGGCC	Genotyping Tet2 mutant mice	This paper
Tet2 KO Gen Fw	CCCATTGTTCTTTGCTCCATGCA	Genotyping Tet2 KO mice KO allele	Zhe et al, Blood 2011
Tet2 KO Gen Rev	CGTCGCCGTCAGCTCGACCAG	Genotyping Tet2 KO mice KO allele	Zhe et al, Blood 2011
Tet2 WT Gen Fw	CCATGCAGGGAAGACAAGAGTAGC	Genotyping Tet2 KO mice WT allele	Zhe et al, Blood 2011
Tet2 WT Gen Rev	ATCTTGTTGGATGGAGCCCAGAG	Genotyping Tet2 KO mice WT allele	Zhe et al, Blood 2011
Tet1 RTqPCR Fw	TGCACCTACTGCAAGAATCG	Real time qPCR	Dawlaty et al, Cell Stem Cell 2011
Tet1 RTqPCR Rev	AAATTGGCATCACAGCTTCC	Real time qPCR	Dawlaty et al, Cell Stem Cell 2011
Tet2 RTqPCR Fw	GTCAACAGGACATGATCCAGGAG	Real time qPCR	Zhe et al, Blood 2011
Tet2 RTqPCR Rev	CCTGTTCCATCAGGCTTGCT	Real time qPCR	Zhe et al, Blood 2011
Tet3 RTqPCR Fw	TCCGGATTGAGAAGGTCATC	Real time qPCR	Dawlaty et al, Develop Cell 2014
Tet3 RTqPCR Rev	CCAGGCCAGGATCAAGATAA	Real time qPCR	Dawlaty et al, Develop Cell 2014
Hoxa9 RTqPCR Fw	ATGGCATTAAACCTGAACCG	Real time qPCR	Ailing et al, JCI 2013
Hoxa9 RTqPCR Rev	GTCTCCGCCGCTCTCATTC	Real time qPCR	Ailing et al, JCI 2013
Gata1 RTqPCR Fw	TGCCTGTGGCTTGATCA	Real time qPCR	Kaimakis et al, Blood 2016
Gata1 RTqPCR Rev	TGTTGTAG GGTCGTTTGAC	Real time qPCR	Kaimakis et al, Blood 2016
Gata2 RTqPCR Fw	AAGCTGCACAATGTAAACAGG	Real time qPCR	Kaimakis et al, Blood 2016
Gata2 RTqPCR Rev	CCTTTCTTGCTCTTCTTGAC	Real time qPCR	Kaimakis et al, Blood 2016
Gapdh RTqPCR Fw	ACATCTCACTCAAGATTGTCAGCA	Real time qPCR	Dawlaty et al, Develop Cell 2014
Gapdh RTqPCR Rev	ATGGCATGGACTGTGGTCAT	Real time qPCR	Dawlaty et al, Develop Cell 2014